

AutoCAD inspired level-set algorithm for 3D simulation of industrial fire and explosion

Hyun-jun Kim, Jack J. Yoh*

Department of Mechanical and Aerospace Engineering, Seoul National University
Seoul, Korea 151-742

1 Introduction

In a conventional method of defining an interface via the level set, an analytic function is required to initialize the material boundary [1]. It is often the case that a realistic material interface is never circular or rectangular, rather it is complex and three-dimensional in its shape. Thus defining and initializing such material interface as a zero level-set has been a great challenge for multi-material hydrodynamic simulation. In this paper, we present a novel interface initialization algorithm for defining a zero level-set for constructing any complex 3D geometry that utilizes STL (Stereolithography) file format [2]. The algorithm is tested in the deflagration spreading problem associated with a complicated plant facility. The gas tank explosion by leakage of hydrocarbons is simulated as a process of catastrophic failure of gas storage in industrial fires.

2 Numerical consideration

2.1 Interfacial algorithm based on the level-set algorithm

The embedded interface Γ in 3D computation domain is defined as the zero level set of the signed distance function, ϕ . The evolution equation [1] for the level set function (1) is given by

$$\frac{\partial \phi}{\partial t} + \vec{V} \cdot \nabla \phi = 0 \quad (1)$$

where the velocity field, \vec{V} is usually given by the external flow. Here, we replace function, ϕ with a new signed distance function developed on the basis of the STL file format rather than the commonly known spherical or cylinder equations. The STL format can be extracted as ASCII or Binary in various CAD programs, and we accessed this algorithm based on ASCII format. Basically, the STL format divides any modeled shape into triangles, providing the position coordinates for the three vertices of each triangle and the normal vector outward looking at the triangles. A method of determining interfaces with an interest to

the STL file format has been reported in [3]. However, we have independently utilized the classification method of Gram-Schmidt Orthogonalization to constrain the triangles on the plane and defining the level value at the grid point in 3D space within the limited triangular column.

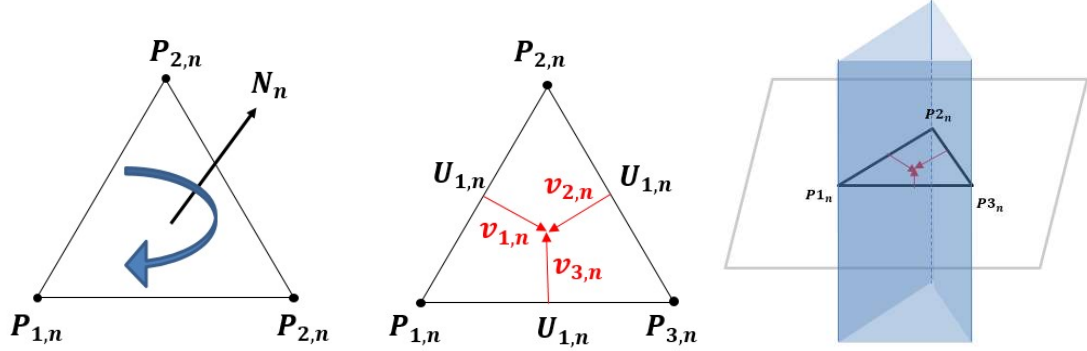


Figure 1. Left: Features of STL format including normal vector information and location of the vertex of a triangle; Center: the vectors $v_{1,n}, v_{2,n}, v_{3,n}$ created by Gram-Schmidt Orthogonalization process with $U_{1,n}, U_{2,n}, U_{3,n}$ vectors; Right: A triangular prism formed by three planes perpendicular to the plane including the triangle in 3D space

Here n is the total number of triangles in geometry divided by STL format. We specify the vertices and the surface outward normal vectors of the triangle as $P_{1,n}, P_{2,n}, P_{3,n}$ and N_n in order as shown in Fig. 1 (left), and create temporary vectors $U_{1,n}, U_{2,n}, U_{3,n}$ as shown in Fig. 1 (center).

$$v_{1,n} = U_{2,n} - \left(\frac{U_{2,n} \cdot U_{1,n}}{U_{1,n} \cdot U_{1,n}} \right) U_{1,n}, \quad v_{2,n} = U_{3,n} - \left(\frac{U_{3,n} \cdot U_{2,n}}{U_{2,n} \cdot U_{2,n}} \right) U_{2,n}, \quad v_{3,n} = U_{1,n} - \left(\frac{U_{1,n} \cdot U_{3,n}}{U_{3,n} \cdot U_{3,n}} \right) U_{3,n} \quad (2)$$

Here $v_{1,n}, v_{2,n}, v_{3,n}$ are temporary vectors that are vertical to each side of the STL triangle generated by Gram-Schmidt orthogonalization using Eq. (2). New planes created by vectors $v_{1,n}, v_{2,n}, v_{3,n}$ and vertices $P_{1,n}, P_{2,n}, P_{3,n}$ surrounding one triangle on the surface of a geometry become a triangular prism, as shown in Fig. 1 (right).

The signed distance function reconstructed from the STL triangular surface replacing ϕ in Eq. (1) is defined by

$$\tilde{\phi}_n(G_k) = (G_k - P_{1,n}) \cdot N_n \quad (3)$$

$$\phi_n(G_k) = \min_n (\tilde{\phi}_n(G_k)) \quad (4)$$

where G_k is grid point of the computation domain, and N_n is the unit normal vector of STL triangle. When a grid point resides in a direction outward from a surface, Eq. (3) becomes a positive-signed level value. However, when it is in the opposite direction, then the negative sign is given. This makes it possible to determine whether the grid point is inside or outside any complex material boundary.

As shown in Fig. 2 (left), the first signed distance of each grid point from any triangular surface, which is restricted by the triangular prism, are automatically identified. Since there may be several triangular surfaces around a grid point, we use Eq. (4) to find the shortest distance and remain one level value at this grid point. A limited triangular prism is set up to identify whether the grid points in upper and lower ranges of the STL triangle are inside or outside the 3D geometry. Therefore, the main idea in 3D shape reconstruction

algorithm is the STL triangle surfaces that are restricted by using a triangular prism within the 3D alignment grid.

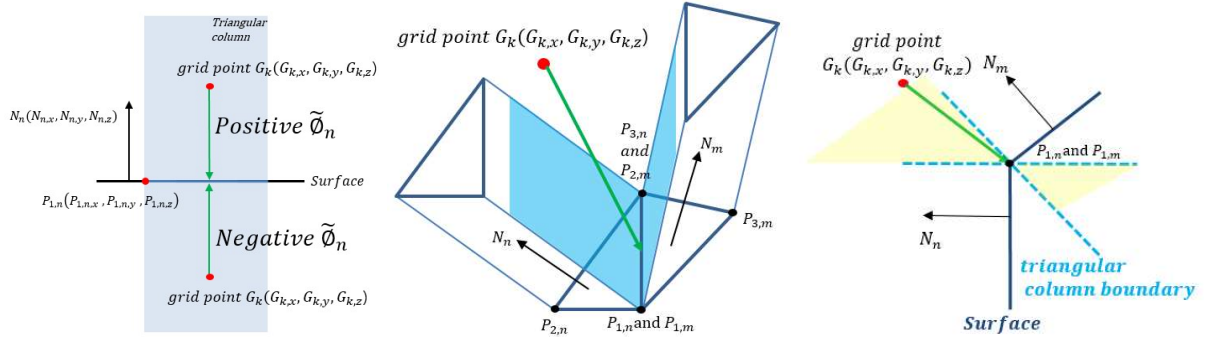


Figure 2. Left: the concept of a distance formation between a grid point and a plane viewed from a side; Center: a case where the grid point is not included in any triangular column of 3D; Right: exceptional case of section view

But there are still exceptional circumstances. In the case of a bended geometry as shown in Fig. 2 (center), the grid point G_k is located outside each restricted triangular column boundary, so no proper level is assigned. Therefore, a second distance function is used to find the shortest distance between the edge and the grid point G_k that meets each triangle. The equation is defined as,

$$\tilde{\phi}_n(G_k) = \frac{\|(P_{3,n} - P_{1,n}) \times (P_{1,n} - G_k)\|}{\|P_{3,n} - P_{1,n}\|} \text{ or } \frac{\|(P_{2,m} - P_{1,m}) \times (P_{1,m} - G_k)\|}{\|P_{2,m} - P_{1,m}\|} \quad (5)$$

Here, $\tilde{\phi}_n(G_k)$ is an equation for obtaining only distance. Eq. (5) summarizes how to find the distance between the line and the point where the n-th triangle and the m-th triangle are two points in space. As the characteristics of the STL, the neighboring triangles share two vertices. So it is possible to calculate the distance by choosing one of the above two expressions. The method of assigning sign to Eq. (6) can be defined as,

$$\text{sign} = \frac{(G_k - P_{1,n}) \cdot N_n}{\|(G_k - P_{1,n}) \cdot N_n\|} \text{ or } \frac{(G_k - P_{1,m}) \cdot N_m}{\|(G_k - P_{1,m}) \cdot N_m\|} \quad (6)$$

In Eq. (6), one of the three vertices of the STL may be used, so that it is represented by an expression for one point. The grid point G_k is made into a vector using one of the vertices of the triangle. Since the normal direction of the surface always faces outward, only sign is left in the result of dot product of two vectors. So, for a grid point G_k not included in a triangular column like Fig. 2 (Right), we can define a second signed distance function using Eq. (5) and (6) as

$$\hat{\phi}_n(G_k) = \min_n \text{sign} * \tilde{\phi}_n(G_k) \quad (7)$$

As in Eq. (4), since there may be several surfaces around the grid point, the shortest signed distance is obtained by using Eq. (7). Once this whole process is performed for all triangles in the STL file in turn, all grid points are given a level value for 3D geometry.

2.2 Equation of state and reaction progress for combustible gas air mixture

The pressure P of combustible gas is calculated by the ideal gas law, $P(\rho, T) = \rho RT$ or $P(e, \rho) = (\gamma - 1)\rho e$. Also, $\dot{\omega}_i \equiv \partial Y_i / \partial t = A \rho Y \exp(-E_a/RT)$, reaction rate is described by experimentally validated first-order Arrhenius kinetics. Here, R , M , Y_i , E_a and γ are universal gas constant, molecular weight, pre-exponential factor, activation energy and specific heat ratio, respectively. Initial conditions of a stoichiometric ethylene-air mixture and Arrhenius kinetic parameters are shown in Table 1.

Table 1: Material properties of Ethylene-air mixture

	ρ_0 (g/m ³)	P_0 (atm)	T_0 (K)	γ	M_w (kg/mol)	A (kg s)	E_a (J/mol)	Q (J/kg)
Ethylene-air [4]	1.58	1	293	1.15	0.029	3.2x10 ⁸	86119.9	4.1014x10 ⁶

For inert structure, the Mie-Gruneisen equation of state (EOS) is adopted to calculate pressure P of stainless steel as,

$$P_{inert\ material} = P_H + \Gamma_0 \rho (e - e_H); \quad V = \frac{\rho_0}{\rho} \quad (8)$$

To calculate the strain of steel, the rate-dependent Johnson-Cook strength model [5] is used and expressed in Eq. (9)

$$\sigma_Y = \left(A_0 + B_0 (\bar{\epsilon}^P)^n \right) \left(1 + C_0 \ln \left(\frac{\dot{\bar{\epsilon}}^P}{\dot{\epsilon}_0} \right) \right) \left(1 - \left(\frac{T - T_0}{T_m - T_0} \right)^m \right) \quad (9)$$

where Γ_0 , s , c_0 , A , B , n and m are material constants, and ρ_0 , T_m and T_0 are initial density, melting temperature and ambient temperature. The material properties and Mie-Gruneisen EOS constants are summarized in Table 2.

Table 2 Mie-Gruneisen EOS and Johnson-Cook model for inert materials

	ρ_0 (kg/m ³)	C_0 (m/s)	S	Γ	A_0 (GPa)	B_0 (GPa)	C_0	m	n
Stainless Steel [5]	7800	4570	1.49	1.93	0.31	0.1	0.07	1	0.65

3 Results

3.1 3D- reconstruction and deflagration spreading

We refer to experimental setting in [6] for modeling the 3D-reconstruction. Figure 3 (Left) is the result of importing Autocad file directly into a 3D level-set reconstruction. The size of the corresponding tank facility is 2m x 8m x 2.5m that includes 8 large and small tanks with support joints and metal frames.

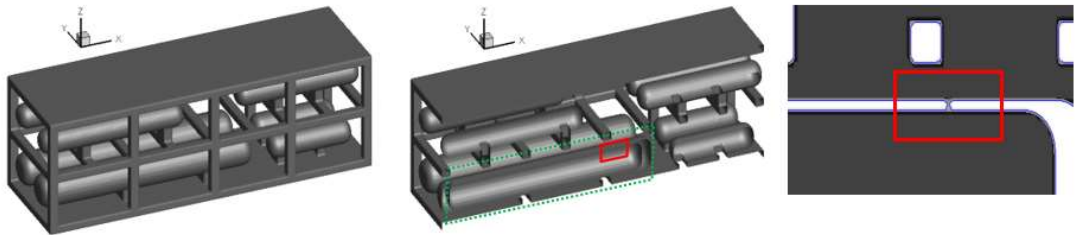


Figure 3. Left: 3D-reconstruction free view; Center: Fuel tank showing internal space (in green dash line) viewed with XZ-plane; Right: Crack formed at tank surface (in red line) viewed in Y-plane

Based on the newly developed algorithm, a zero level-set value is set such that the distinction between inside and outside is naturally considered. As shown in Fig. 3 (Center), the wall thickness of a tank is modeled as 50 mm. The figure on the right shows a crack of 10 mm in width, which is not visible on the outer wall of the tank. The ethylene-air flame in stoichiometric condition leaks and spreads from a crack opening and is seen to grow into a large fire.

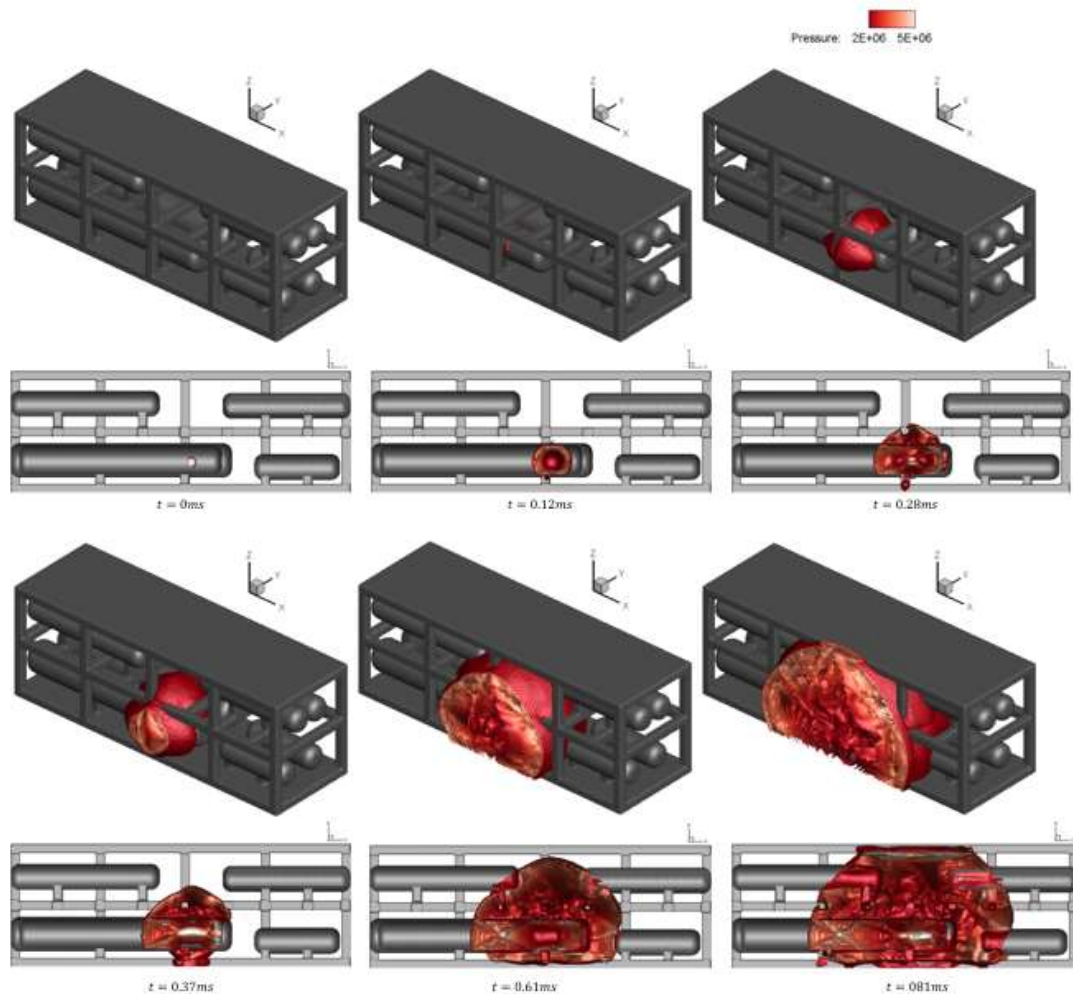


Figure 4. Isosurface contour for flame propagation shape according to each time. First and third row: free view; Second and forth row: section view with XZ-plane

Figure 4 shows the spreading over entire facility at each time delay. At $t = 0.12$ ms, it was confirmed that the flame developed inside the tank started to break through the crack. Thereafter, it can be seen that deflagration spreads to the entire structure.

3.2 Wall deformation by deflagration spreading

The crack on the wall of the tank was observed as shown in Fig. 5 (Top). The width of initial crack was 10 mm, and it reached up to 80 mm as the reaction progressed. Over time, it was also confirmed that deflagration increases pressure and deforms columns of the structure in the plant facility.

As a result, Eulerian based hydrodynamic code is equipped with a CAD-inspired level-set approach that is reliable for simulating any complex geometry. Various fuels will be tested at wide variety of real plant scenarios in the future.

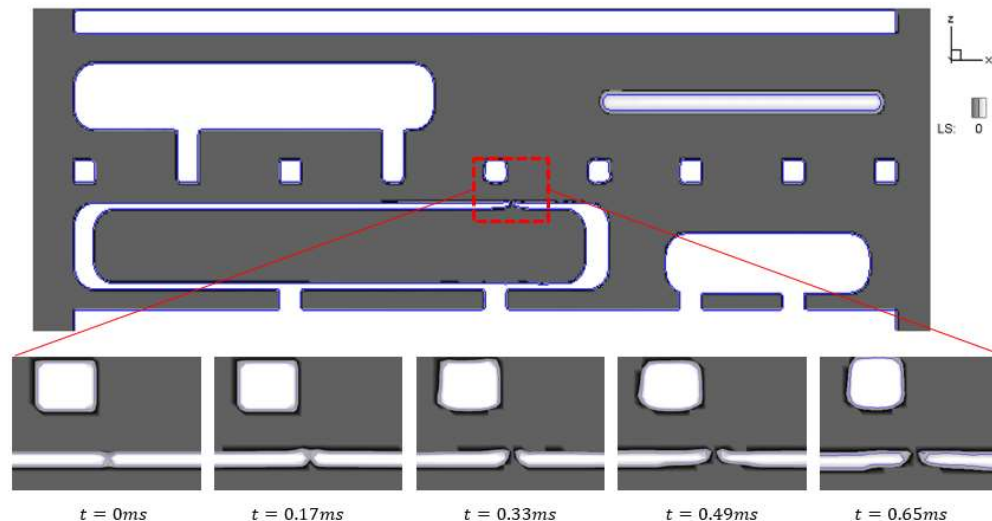


Figure 5. Top: the structure cutting view with Y-plane. Bottom: Crack width changes with time step

ACKNOWLEDGMENTS

This work was financially supported by Agency for Defense Development contracted through IAAT at Seoul National University.

References

- [1] Kim KH, Gwak MC, Yoh JJ. (2015). An enhanced particle reseeding algorithm for the hybrid particle level set method in compressible flows. *J. Sci. Comput.* 65: 431.
- [2] Szilvsi-Nagy M, Matyasi GY. (2003). Analysis of STL files. *Math. Comput. Model.* 38: 945.
- [3] Choi JI, Oberoi RC, Edwards JR, Rosati JA. (2007). An immersed boundary method for complex incompressible flows. *J. Comput. Phys.* 224: 757.
- [4] Gwak MC, Yoh JJ. (2013). Effect of multi-bend geometry on deflagration to detonation transition of a hydrocarbon-air mixture in tubes. *Int. J. Hydrogen Energ.* 38: 11446
- [5] Gwak MC, Lee YH, Yoh JJ. (2016). Numerical Investigation of Kerosene-Based Pulse-Detonation Loading on the Metal Tubes. *J. Propul. Power*, 1146
- [6] Hjertager BH, Fuhre K, Bjørkhaug M. (1988). Gas explosion experiments in 1: 33 and 1: 5 scale offshore separator and compressor modules using stoichiometric homogeneous fuel/air clouds. *J. Loss. Prevent. Proc.* 1: 197.